Endovascular Aneurysm Repair Using Anaconda Repositionable Aortic Stent Graft Assisted Exclusively by Intravascular Ultrasound Imaging

Gaetano La Barbera, Giuliana La Rosa, Fabrizio Valentino, Gabriele Ferro, Dario Parsaei, Rosario Lipari, Davide Petrucelli and Francesco Talarico

Vascular Surgery Department, Civic Hospital of Palermo, Palermo, Italy

Abstract

Arteriography with contrast medium (CM) injection is normally employed to visualise the lowest renal artery during endovascular aneurysm repair (EVAR). Intravascular ultrasound (IVUS) has been proposed as an alternative, real-time imaging diagnostic technique to arteriography. In this study, we evaluated the feasibility of EVAR using Anaconda repositionable aortic stent graft (Vascutek) assisted by IVUS (Volcano Visions, Philips) during intraluminal navigation without CM. From January 2016 to December 2017, 25 patients with infrarenal abdominal aortic aneurysms, identified through anatomical inclusion criteria, underwent EVAR. All of the patients had an arteriogram at the end of the EVAR procedure to confirm aortic stent graft patency and to exclude type 1 endoleaks. The primary objective was the technical and clinical success of this CM-free aortic stent graft delivery procedure. At the end of the period, 150 target vessels were evaluated. IVUS versus angio-CT sensitivity and specificity rate were 97.3% and 100%, respectively. The primary technical success was obtained in 88% of the cases. Three patients (12%) needed CM injection to complete the procedure and there were no cases of type 1 endoleak. Primary clinical success was 100%. During follow-up at a mean of 20 months, none of the patients died or had complications. We conclude that a full EVAR procedure is feasible using only IVUS navigation and repositionable aortic stent graft without CM injection in anatomically selected cases.

Keywords

Intravascular ultrasound, abdominal aortic aneurysm, iodinated contrast medium, endovascular aneurysm repair

Disclosure: The authors have no conflicts of interest to declare.
Received: 28 January 2019 **Accepted:** 13 February 2019 **Citation:** *Vascular & Endovascular Review* 2019;2(1):32–7. **DOI:** https://doi.org/10.15420/ver.2019.3.1
Correspondence: Gaetano La Barbera, Vascular Surgery Unit, Ospedale Civico Di Cristina Benfratelli, 4 Piazza N Leotta, 90127, Palermo, Italy.
E: gaetano.labarbera@yahoo.com

Endovascular aneurysm repair (EVAR) has been employed in nearly 70% of aneurysm treatments over the past decade because of its low invasiveness.[1] During EVAR, the precise visualisation of the lowest renal artery (LoRA) and the hypogastric artery (HA) is fundamental for the correct delivery of both the aortic stent graft (ASG) body and Iliac limbs. The visualisation of the LoRA and HA are normally obtained by the injection of a contrast medium (CM), which can cause renal function impairment, acute adverse reactions and requires X-ray exposition.[2] In this study, we evaluated the feasibility of EVAR using only intravascular ultrasound (IVUS) imaging navigation. Since this was a new technique, we decided to employ a repositionable ASG to ensure LoRA patency at the end of the procedure.[3]

IVUS has been proposed as an imaging diagnostic technique that can provide useful information during endovascular stent graft repair.[4,5] Unlike traditional arteriography, IVUS provides the real-time visualisation of the vascular findings.[6] However, a clear indication of what information can be obtained by IVUS during EVAR procedures is still missing.[7,8]

Materials and Methods

From January 2016 to December 2017, 130 patients with infrarenal atherosclerotic abdominal aortic aneurysm (AAA) were treated by EVAR in our tertiary vascular referral hospital. Of these, 25 patients (22 men and three women) were enrolled in a registry for a monocentric, non-randomised, open label study. The protocol was approved by the hospital's institutional review board and every patient gave informed consent for the procedure. The patient data were gathered prospectively and analysed retrospectively. We used the Anaconda repositionable ASG (Vascutek). Intraluminal arterial navigation was assisted with IVUS using the Volcano Visions PV 0.035 catheter-based system (Philips).

Study Design

We considered eligible patients with infrarenal AAA. The anatomy of the aneurysm was defined according to Eurostar classification.[9] Preoperative assessment consisted of a clinical examination including the Society of Vascular Surgery/International Society of Cardiovascular Surgery risk scores and the American Society of Anaesthesiologists classification.[10,11] The inclusion and exclusion criteria are listed in *Table 1*. Iliac axis tortuosity was considered according to the definition of Taudorf et al.[12] CT angiography (CTA) was the standard preoperative imaging modality to assess for endograft sizing and aneurysm repair. All CTA sequences were processed using a 3D centre-line reconstruction by 3Surgery™ 4.0 platform (3mension Medical Imaging).

Study Hypothesis

The aim of this study was to evaluate the technical feasibility and clinical success according to Chaikof's definition of EVAR.[13] IVUS was used for vascular navigation and replaced intraprocedural angiography for target artery visualisation for the coeliac trunk, superior mesenteric, renal arteries and HA, as well as ASG delivery. We considered a target artery correctly visualised if, at its origin, the hyperechoic image of the aortic wall and the target artery wall were both clearly visualised, separated by the hypoechoic blood appearance at its lumen. We did not perform an arteriogram to aid positioning of the ASG except when IVUS was associated with no clear imaging of the ostium of the target arteries and at the end of the EVAR to check both the patency and the sealing of the ASG.

The technical and clinical success defined as ASG delivery assisted only by IVUS were considered the primary endpoints. The technical success is represented by: the delivery of the ASG just below the inferior edge of the LoRA allowing its patency; the correct patency of the ASG with adequate distal perfusion; the patency of the HA origin after the limbs deployment; and absence of any type 1 endoleak. The clinical success was defined by the absence of adverse events and a 30-day survival rate. We considered the amount of CM and the procedure duration for each patient as secondary endpoints.

Aortic Stent Graft

The Anaconda ASG is a three-piece endovascular system. The stents are made of multiple-element nitinol stents internally covered with woven polyester fabric. The top of the ASG consists of a dual-ring stent that looks like an anaconda's mouth. The configuration we used has anterior and posterior peaks and two valleys on the right and left side.[3] The proximal stent is anchored in an infrarenal position by four pairs of nitinol hooks. The iliac legs are supported with independent nitinol ring stents, preventing kinks and providing flexibility for fixation in femoroiliac anatomy. The Anaconda ASG system can be repositioned by the control collar of the delivery system handle. Engagement of the contralateral gate is facilitated by a preloaded magnet wire to assist in the cannulation of the contralateral limb.

Intravascular Ultrasound

The Volcano Visions PV 0.035 IVUS catheter-based system is an over-the-wire intravascular imaging catheter with a digital ultrasound transducer at the distal end. It acquires axial images of the vessel from inside the artery, providing detailed and accurate measurements of the lumen, arterial segment length, plaque area, and the location of key anatomical landmarks. There are 25 radiopaque markers on the distal end of the catheter starting 1 cm from the imaging plane. A lubricious hydrophilic coating is applied externally to the catheter.

Operative Procedure

All surgeries were performed with a radiolucent table under fluoroscopic guidance. The ASG size was selected according to the AAA anatomy, with 20–30% oversizing of the prosthetic body in relation to the infrarenal neck diameter. All patients had a percutaneous procedure with local anaesthesia and intraprocedural anticoagulation. After placing a 10 Fr Avanti+® introducer (Cordis) on both sides, a stiff Lunderqvist 0.035 guidewire (Cook Medical) was advanced to the aortic arch. Then the IVUS catheter was moved over the left guidewire up to the coeliac trunk. Recording the scan, the coeliac trunk, the superior mesenteric and the renal arteries (RRAA) were identified. We then focused on the RRAA. The IVUS tip was positioned at the LoRA origin

Table 1: Inclusion and Exclusion Criteria

Inclusion criteria	Exclusion criteria
• Aged 18–85 years • Available to complete follow-up • Life expectancy >2 years • Candidate for open surgery • AAA >50 mm in diameter • Infrarenal proximal neck diameter 18–31.5 mm • Infrarenal proximal neck length ≥15 mm • Distal iliac fixation site diameter <16 mm • Distal iliac fixation site length >30 mm • Access vessel >7.5 mm in diameter	• Ruptured or symptomatic AAA • Juxta-, para- or suprarenal AAA • ASA grade IV or V • Known allergy to CM, nitinol or polyester • Impossibility to preserve at least one hypogastric artery • Presence of VVAA or RRAA atherosclerotic disease • Alpha angle ≥60° • Beta angle ≥60° • >50% continuous aortic neck calcification • >50% continuous aortic neck thrombus • Reverse conical infrarenal aortic neck • External iliac stenosis >30%

AAA = abdominal aortic aneurysm; Alpha angle = angle between the longitudinal axis of the suprarenal aorta and the infrarenal aortic neck; ASA = American Society of Anaesthesiologists; Beta angle = angle between the longitudinal axis of the infrarenal aortic neck and the anevrismal sac; CM = contrast medium; RRAA = renal arteries; VVAA = visceral arteries.

Figure 1: Lowest Renal Artery Level Origin

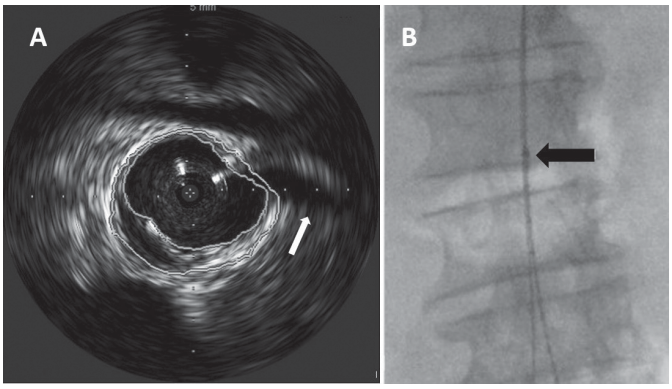

A: Clear visualisation of the left renal artery as the lowest renal artery (white arrow) on intravascular ultrasound scan. B: On X-ray, the intravascular ultrasound tip corresponds to the lowest renal artery level origin and proximal landmark of the aortic stent graft body delivery (black arrow).

and we marked this point as the proximal landmark of ASG delivery on the X-ray (*Figure 1*).

Watching the ostium of the LoRA on the IVUS screen in real-time and the corresponding level of the IVUS tip on the X-ray screen, the ASG device was moved up from the right groin and it was then delivered, checking its position on the X-ray screen and taking care not to overcome the IVUS tip. Then we cannulated the contralateral gate of the body.

Once we positioned the stiff guidewire inside the ASG body from the left groin, the IVUS catheter was advanced to check the patency of the LoRA. If IVUS did not visualise the LoRA, this meant that the ASG body covered it. In this case, the X-ray showed that the proximal ring of the ASG was over the tip mark of the IVUS catheter (*Figure 2*). We then collapsed the ASG body, moving it down and releasing it, to keep the LoRA origin clear. We checked with IVUS again that the LoRA was clearly visualised (*Figure 3*). Then we moved down the IVUS catheter until we visualised the hypogastric ostium. We marked the distal

Figure 2: Proximal Aortic Stent Graft Body Delivery

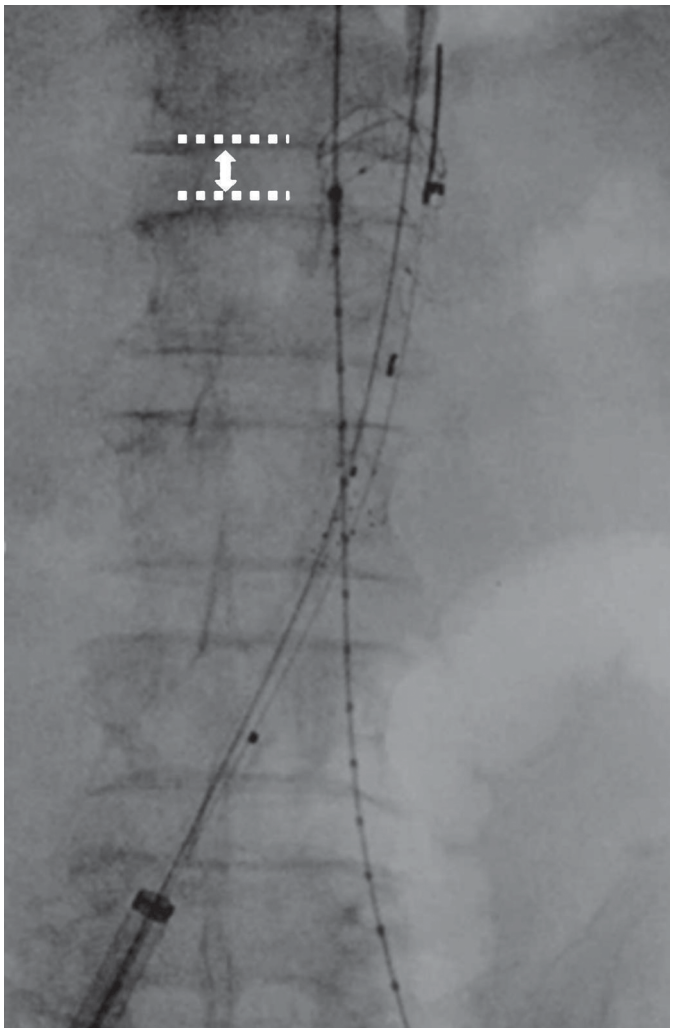

Image on the X-ray screen showing the proximal aortic stent graft stent overcoming the intravascular ultrasound tip (white arrow).

landing zone by placing the IVUS tip above this level (*Figure 4*). We then measured the length of the corresponding limb and released it using the CM-marked IVUS catheter segment. We repeated the last step for the right limb.

Follow-up

Each patient underwent postoperative CTA at discharge. An abdominal instrumental follow-up was performed using CTA, duplex scan or contrast-enhanced ultrasonography (CEUS) at 6, 12 and 24 months. We registered overall survival, death as a result of aneurysm-related treatment, open repair conversion, endoleaks, reintervention, aneurysm sac expansion or rupture, renal artery occlusion, stent-graft and arterial thrombosis, ASG integrity and migration.

Statistical Analysis

The 2 × 2 table method analysis was employed to characterise the IVUS versus CTA accuracy, to clearly visualise target vessel location. Statistical significance of correlations was tested with the Pearson correlation coefficient.

Results

Patient characteristics are listed in *Table 2*. The mean age of the participants was 74.1 years (range 58–85). We analysed 150 target

Figure 3: Intravascular Ultrasound-directed Aortic Stent Graft Body Repositioning

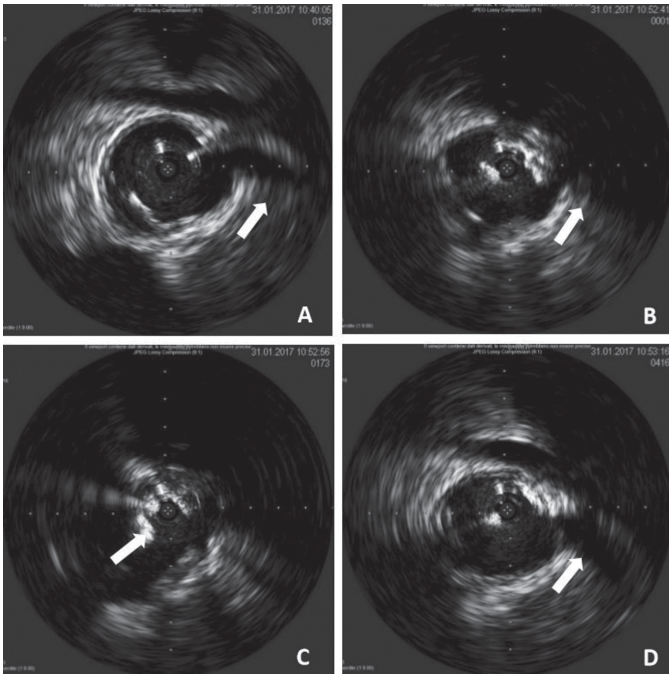

A: Lowest renal artery (LoRA) before aortic stent graft (ASG) delivery (white arrow). B: LoRA disappearance after ASG delivery (white arrow). C: ASG collapse aimed at body repositioning (white arrow). D: LoRA reappearance after ASG repositioning (white arrow).

Figure 4: Marking the Distal Landing Zone

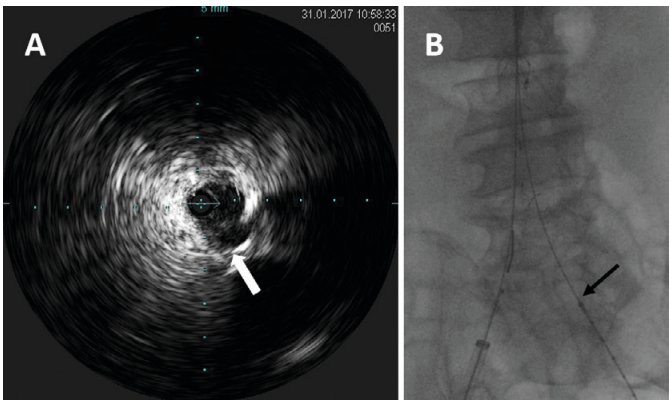

A: Intravascular ultrasound screen shows clear visualisation of the hypogastric artery origin (white arow). B: On X-ray screen, the intravascular ultrasound tip corresponds to the distal landmark of iliac limb delivery (black arrow).

vessels. IVUS and preoperative CTA findings for the visualisation of visceral arteries (VVAA) matched in 100% of patients.

Postoperative Technical and Clinical Success

In terms of RRAA visualisation, IVUS and preoperative CTA findings, matched in 84% of patients. In four patients (16%), IVUS was not able to clearly visualise the left renal artery (LRA), so we needed to use arteriography by injecting 30 ml of CM for each patient. In two cases the beta angle (the angle between the longitudinal axis of the infrarenal aortic neck and the anevrismal sac) was >40° and the LRA was the LoRA. In the other two cases, the controlateral guidewire competed with ultrasound beam; one of them had a beta angle >40° and the LRA was the LoRA. Therefore, because only three patients required CM for LoRA visualisation for ASG delivery, we obtained 88% technical success.

Table 2: Patient Characteristics

Demographic		Mean or occurrence (n=25)	Range or percentage
Age		74.1 years	58–94 years
Sex	Male	n=22	88%
	Female	n=3	12%
ASA score	I	n=0	0%
	II	n=18	72%
	III	n=7	28%
Risk factors	Diabetes	n=2	8%
	Smoking	n=2	8%
	Hypertension	n=23	92%
	Hyperlipidaemia	n=11	44%
	Ischaemic cardiac disease	n=8	32%
	Pulmonary disease	n=9	36%
Eurostar type of AAA	A	n=22	88%
	B	n=3	12%
Shape of AAA	Fusiform	n=23	92%
	Saccular	n=2	8%
Diameter infrarenal neck	Top	23 mm	18–30 mm
	Middle	24.5 mm	20– 28 mm
	Bottom	26 mm	25–29 mm
Shape of neck	I I	n=22	88%
	\ /	n=1	4%
	< >	n=2	8%
	> <	n=0	0%
Length of neck		20 mm	15–35 mm
Angulation of neck	≤40°	n=21	84%
	>40°	n=4	16%
Diameter of AAA		5.8 mm	50–75 mm
Diameter of common iliac	Left	12 mm	7–18 mm
	Right	13 mm	7–18 mm
Length of common iliac		45 mm	30–55 mm
Pelvic artery index of tortuosity		1.4	1.1–1.5

AAA = abdominal aortic aneurysm; ASA = American Society of Anaesthesiologists.

At the end of the EVAR procedure, we always made an arteriography by injecting 15 ml of CM, confirming the patients had the correct ASG patency and no type 1 endoleak. In a single patient, one of the HA origins was not clearly visualised because of ostium calcification. We did not perform a control arteriogram on this patient. The 2 × 2 table analysis for evaluating the accuracy of IVUS to clearly visualise VVAA, RRAA, and HA showed a sensitivity of 97.3% and a specificity of 100%.

The final control arteriogram confirmed the effectiveness of the ASG delivery with the correct patency of ASG, VVAA, HA and LoRA, as well as arterial outflow. The postoperative course was uneventful and all the patients were discharged. The average postoperative hospital stay was 2 days (range 1–3 days).

Contrast Medium Amount and Procedure Duration

The average CM employed for the population study was 19.8 ml (range: 15–45 ml). Concerning the visualisation of the LoRA, we compared the amount of CM employed with the aortic neck angle. Three patients with a beta angle >40° received 30 ml of CM. Conversely, 21 of the 22 patients with a beta angle ≤40° received less than 30 ml of CM. Therefore the amount of CM employed was significantly correlated with the beta angle (p<0.01; *Figure 5*).

Figure 5: Amount of Contrast Medium Received and Beta Angle

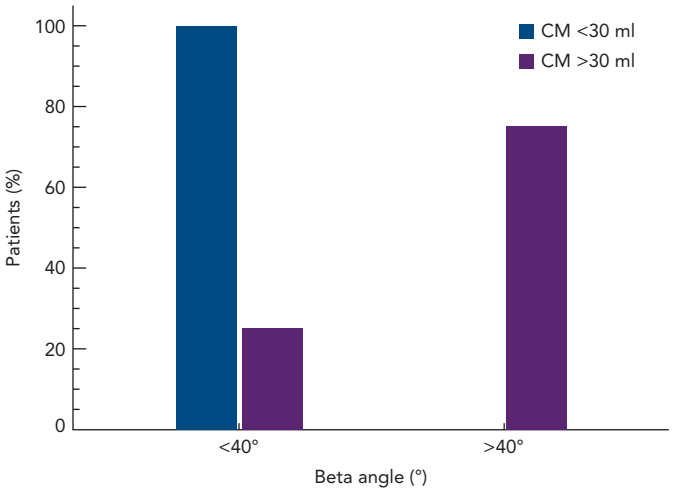

Istogram showing the percentage of patients who received contrast medium <30 ml (blue) or contrast medium >30 ml (violet) with a beta angle <40° or >40° Patients with a more regular aortic neck angle (<40°), received significantly less contrast medium (p<0.01). CM = contrast medium.

In 68% of the patients, the ASG body was repositioned after the first delivery because the proximal ring of the ASG body competed with the LoRA. There was no type 1 endoleak, and one patient had a type 2 endoleak due to two understated lumbar arteries. The average EVAR time was 137 minutes (range 95–170 minutes, standard deviation 25.5 minutes).

Short- and Mid-term Clinical Success

The follow-up range was an average of 20 months with a range of 1–24 months, during which none of the patients had died. The patient discharged with type 2 endoleak was asymptomatic, and the scheduled ultrasound controls showed a stable aneurismal diameter. During the follow-up, none of the patients had open repair conversion, new endoleaks, AAA sac expansion or rupture, renal artery occlusion, reintervention, thrombosis, loss of ASG integrity or ASG migration.

Discussion

Until recently, IVUS has been used to support imaging techniques in peripheral arterial revascularisation, mostly in the coronary and carotid areas.[4–8,14–18] IVUS is usually used as an ancillary intraprocedural technique during EVAR to visualise the target vessel compared with the more standard use of CM arteriography.[14,19] It has not been clear whether IVUS can efficiently replace arteriography. Our study, with a mean follow-up of 20 months has proved the technical feasibility of a complete EVAR performed with Anaconda repositionable ASG and vascular navigation assisted only by IVUS.

A study by Knowles et al. found that IVUS accuracy for target vessel location had a sensitivity of 100% in juxtarenal AAA for the location of both VVAA and RRAA.[14] Our study focused on infrarenal AAA and we found 97.3% sensitivity and 100% specificity for VVAA and RRAA

visualisation. Some authors emphasise the importance of the aortic neck angle related to the accuracy of IVUS imaging. It has been found that the placement of the IVUS probe within the lumen of an angulated aortic neck can result in an increased echogenic signal in the wall closest to the array, an attenuation of the signal on the opposite wall, and an overestimation of vessel size.[6]

Our 88% postoperative technical success rate suggests that the more regular the AAA anatomy, the more accurate the IVUS imaging. We found that IVUS did not visualise the LoRA in cases where the beta angle was >40°. We can conclude from this that IVUS correctly visualises the LoRA if the beta angle is not critical and if the echogenic tip is in the appropriate position for ultrasonic irradiation.

As already found in previous studies, the endoluminal, centre-lined position of the IVUS is the best condition for the most accurate imaging.[6,20] If the IVUS catheter tip is excessively dislocated toward one side of the aortic wall, the stiff guidewire support can be improved with a 30 cm, 9 Fr sheath advanced to the level of the left renal vein, as reported by Arko et al.[21]

Some studies completed EVAR without any final arteriographic information about the correct AAA exclusion. At the end of the procedure, IVUS is employed to confirm the effective ASG delivery and target artery patency, but without using repositionable ASG there is not a possibility to correct the implantation. Using this approach, Segesser et al., in a study involving 80 patients, reported a 5% rate of conversion to open surgery, a 16% rate of endoleak at the discharge and a 2.5% rate of late conversions.[22] Marty et al. reported a 22% rate of major morbidity in a 30-day follow-up period.[7]

Thanks to the use of a repositionable device, our procedure guaranteed the correct placement of the ASG without injection CM and none of the participants had a type 1 endoleak. Concerning the amount of CM used, Hoshina et al. and Knowles et al. always used an arteriogram to confirm the target vessel location and the effectiveness of EVAR.[14,19] In these cases, IVUS imaging reduced the amount of CM injected (67 ± 34 ml versus 123 ± 50 ml; p<0.01).

In our experience, the average CM employed for each patient was significantly lower (19.8 ± 9.3 ml), because in cases with favourable anatomical characteristics we used CM only for the final arteriogram after the EVAR procedure was complete.

ASG body delivery is the pivotal step in EVAR, and IVUS is usually employed passively. Some authors identify the proximal landmark level by IVUS and then marked the level of IVUS tip on X-ray screen.[7,14,22] Then they delivered the ASG under fluoroscopic control. Unlike our technique, they do not have the real-time visualisation of the LoRA and therefore the correct level of the IVUS tip. In our study, the synchronised use of IVUS and repositionable ASG, checks LoRA patency during ASG delivery in an 'active' way, ensuring correct proximal ASG anchoring. We had to reposition the ASG in 68% of patients in our study because of unclear LoRA visualisation. In all these cases it was evident on the X-ray screen that the proximal ASG stent had overcome the IVUS tip (*Figure 2*), indicating a competion with the LoRA. We had to reposition the ASG most frequently during the initial phases of our research, suggesting there is a learning curve with the technique that may affect success. ASG repositioning was needed when there was an upward dislocation of the IVUS tip due to its friction with the ASG device shaft during its advancement, or when there was a misalignment of the proximal edge of the ASG during its delivery. These drawbacks were successfully fixed by repositioning the ASG in a downward fashion.

HA visualisation is the distal landmark. In our experience, IVUS always clearly visualised the origin of the HA, except in one patient because of arterial wall calcifications. Preoperative sizing identifies the HA origin, the calcifications, the percentage of stenosis, the haemodynamic relevance of the hypogastric blood flow and the distance between the aortic bifurcation and the HA origin necessary for measuring the length of the Iliac limb. The intraoperative positioning of the tip of the CM-marked IVUS catheter at the level of the aortic bifurcation allows the level of the HA origin to be measured. If we deliver the Iliac limb a few millimetres above this level, we can ensure that there is no competition with the HA ostium.

Operator dependency is the recognised drawback of using ultrasound as a diagnostic technique.[23] The same holds for IVUS imaging, with the additional caveat that this type of vascular visualisation is not commonly used by vascular surgeons.

Our mean procedure time was 137 minutes, which is comparable to infrarenal standard EVAR, showing that using IVUS imaging does not increase the time of the procedure.[24]

This is a feasibility study and if these preliminary results are confirmed by other studies, IVUS technology development could improve vascular navigation by coupling better imaging with accurate haemodynamic information about the aorta and its branches.

Conclusion

In this preliminary study we performed EVAR using active IVUS in real-time, allowing continuous imaging of the interactions between ASG and LoRA. We showed that CM-free, precise ASG delivery can be performed by using a repositionable ASG. We always performed a completion arteriogram at the end of the EVAR to check the patency of the ASG, excluding any type 1 endoleak and ensuring the effectiveness of the whole procedure. Our results indicate that well-defined inclusion criteria allow the best IVUS target vessel visualisation for CM-free ASG delivery. IVUS imaging is an operator-dependent technique and operator capability increased with experience. This study shows that Intravascular ultrasound technology can make EVAR a less invasive and safer procedure. ■

1. Mani K, Lees T, Beiles B, et al. Treatment of abdominal aortic aneurysm in nine countries 2005–2009: a vascunet report. *Eur J Vasc Endovasc Surg* 2011;42:598–607. https://doi.org/10.1016/j.ejvs.2011.06.043; PMID: 21775173.
2. Nguyen BN, Neville RF, Rahbar R, et al. Comparison of outcomes for open abdominal aortic aneurysm repair and endovascular repair in patients with chronic renal insufficiency. *Ann Surg* 2013;258:3949. https://doi.org/10.1097/SLA.0b013e3182a15ada; PMID: 24022432.
3. Rödel SGJ, Geelkerken RH, Prescott RJ, et al. The Anaconda AAA stent graft: 2-year clinical and technical results of a multicentre clinical evaluation. *Eur J Vasc Endovasc Surg* 2009;38:732–40. https://doi.org/10.1016/j.ejvs.2009.08.007; PMID: 19775918.
4. Ohki T. Pros and cons of IVUS imaging for endovascular procedures. *Endovascular Today* 2008;3:80–2. Available at: https://evtoday.com/2008/03/EVT0308_12.php (accessed 15 February 2019).
5. Clark DJ, Lessio S, O'Donoghue M, et al. Safety and utility of intravascular ultrasound-guided carotid artery stenting. *Cathet Cardiovasc Interv* 2004;63:355–62. https://doi.org/10.1002/ccd.20188; PMID: 15505835.
6. Pearce BJ, Jordan Jr WD. Using IVUS during EVAR and TEVAR: improving patient outcomes. *Semin Vasc Surg* 2009;22:172–80. https://doi.org/10.1053/j.semvascsurg.2009.07.009; PMID: 19765528.
7. Marty B, Tozzi P, Ruchat P, et al. Systematic and exclusive use of intravascular ultrasound for endovascular aneurysm repair – the Lausanne experience. *Interact Cardiovasc Thoracic Surg* 2005;4:275–79. https://doi.org/10.1510/icvts.2004.094193; PMID: 17670408.
8. Phade SV, Toca MG, Kibbe MR. Techniques in endovascular aneurysm repair. *Inter J Vasc Med* 2011:964250. https://doi.

org/10.1155/2011/964250; PMID: 22121487; PMID: 22121487.
9. Harris PL, Buth J, Mialhe C, et al. The need for clinical trials of endovascular abdominal aortic aneurysm stent-graft repair: the EUROSTAR project: EUROpean collaborators on Stent-graft Techniques for Abdominal aortic aneurysm Repair. *J Endovasc Surg* 1997;4:72–7. https://doi.org/10.1583/1074-6218(1997)004<0072:TNFCTO>2.0.CO;2; PMID: 9034923.
10. Rutherford RB, Baker JD, Ernst C, et al. Recommended standards for reports dealing with lower extremity ischemia: revised version. *J Vasc Surg* 1997;26:517–38. https://doi.org/10.1016/S0741-5214(97)70045-4; PMID: 9308598.
11. Wolters U, Wolf T, Stutzer H, Schroder T. ASA classification and perioperative variables as predictors of postoperative outcome. *Br J Anaest* 1996;77:217–22. https://doi.org/10.1093/bja/77.2.217; PMID: 8881629.
12. Taudorf M, Jensen LP, Vogt KC, et al. Endograft limb occlusion in EVAR: iliac tortuosity quantified by three different indices on the basis of preoperative CTA. *Eur J Vasc Endovasc Surg* 2014;48:527–33. https://doi.org/10.1016/j.ejvs.2014.04.018; PMID: 24878235.
13. Chaikof EL, Blankensteijn JD, Harris PL, et al. Reporting standards for endovascular aortic aneurysm repair. *J Vasc Surg* 2002;35:1048–60. https://doi.org/10.1067/mva.2002.123763; PMID: 12021727.
14. Knowles M, Stanley GA, Baig MS, et al. Accuracy and utility of intravascular ultrasound for fenestrated endovascular aortic aneurysm repair. *J Vasc Surg* 2013;58:1157. https://doi.org/10.1016/j.jvs.2013.07.076.
15. Guo BL, Shi ZY, Guo DQ, et al. Effect of intravascular ultrasound-assisted thoracic endovascular aortic repair for 'complicated' type B aortic dissection. *Chin Med J (Engl)* 2015;128:2322–9. https://doi.org/10.4103/0366-6999.163386; PMID: 26315080.
16. Kang SJ, Minitz GS. Outcomes with intravascular ultrasound-guided stent implantation: a metaanalysis of randomized trials in the era of drug-eluting stents. *J Thorac Dis* 2016;8:E841–3. https://doi.org/10.21037/jtd.2016.07.72; PMID: 27619165.
17. Partovi S, Ghoshhajra BB, Walker TG. Beyond stenotic degree assessment in carotid atherosclerotic lesions: single catheter near-infrared spectroscopy and intravascular ultrasound. *Int J Cardiovasc Imag* 2016;32:201–3. https://doi.org/10.1007/s10554-015-0729-4; PMID: 26245472.
18. Karacsonyi J, Alaswad K, Jaffer FA, et al. Use of intravascular imaging during chronic total occlusion percutaneous coronary intervention: insights from a contemporary multicenter registry. *J Am Heart Assoc* 2016;5:e003890 https://doi.org/10.1161/JAHA.116.003890; PMID: 27543800.
19. Hoshina K, Kato M, Miyahara T, et al. A retrospective study of intravascular ultrasound use in patients undergoing endovascular aneurysm repair: its usefulness and a description of the procedure. *Eur J Vasc Endovasc Surg* 2010;40:559–63. https://doi.org/10.1016/j.ejvs.2010.07.018; PMID: 20739201.
20. Geselschap JH, Heilbron MJ, Hussain FM, et al. The effect of angulation on intravascular ultrasound imaging observed in vascular phantoms. *J Endovasc Surg* 1998;5:126–33. https://doi.org/10.1583/1074-6218(1998)005<0126:TEOAOI>2.0.CO;2; PMID: 9633956.
21. Arko FR, Murphy EH, Davis CM 3rd, et al. Dynamic geometry and wall thickness of the aortic neck of abdominal aortic aneurysms with intravascular ultrasonography. *J Vasc Surg* 2007;46:891–7. https://doi.org/10.1016/j.jvs.2007.06.030; PMID: 17980275.
22. Segesser LK, Marty B, Ruchat P, et al. Routine use of intravascular ultrasound for endovascular aneurysm repair: angiography is not necessary. *Eur J Vasc Endovasc Surg* 2002;23:537–42. https://doi.org/10.1053/ejvs.2002.1657; PMID: 12093071.
23. Mansour A. Physician qualification in the clinical diagnostic vascular laboratory. In: AbuRhama AF, Bandick DF (eds). *Noninvasive Vascular Diagnosis: A Practical Guide to the Therapy*. New York: Springer, 2013;11–5.
24. Lee CH, Chang CJ, Huang JK, Yang TF. Clinical outcomes of infrarenal abdominal aortic aneurysm that underwent endovascular repair in a district general hospital. *J Thorac Dis* 2016;8:1571–6. https://doi.org/10.21037/jtd.2016.06.30; PMID: 27499945.